

Formation of Shore-Normal Grooves (Gutters) in Sandstone by Wave Action

Jon Williams¹, Paul Carling², Julian Leyland² and Lucian Esteves³

¹ Mott MacDonald, Croydon, UK. jon.williams@mottmac.com

² University of Southampton, Southampton, UK.

³ University of Bournemouth, Bournemouth, UK.

Abstract

Regularly spaced incised shore-normal grooves (gutters) on plane consolidated surfaces in littoral and sub-littoral zones are widely observed in the marine geological record. Despite their common occurrence there are few investigations into their origins in contemporary marine environments. While their formation is often attributed to wave-induced currents related to wave swash and backwash on the beach-face, no conceptual model has been advanced to explain the presence of gutters, their morphology or their quasi-regular alongshore spacing. The paper examines gutters cut in soft sandstone at Medmerry near Selsey, UK and argues that their formation is related to wave breaking and swash zone processes during an unprecedented sequence of storms in the winter of 2013/14. During this period exceptionally high near-shore waves (H_s around 6m) were recorded for the south coast beaches and these storm conditions persisted periodically through to mid-February 2014. The consequence was extensive beach erosion and the exposure of underlying substrates. In this study gutter morphology was quantified using terrestrial lidar and a wave-resolving numerical model was used to define the nearshore wave conditions and swash characteristics. Three of the largest storm events during the winter of 2013/14 were modelled: (a) moderate waves coincident with an exceptionally high tide; (b) exceptionally high waves occurring during neap tides; and (c) high waves occurring during spring tides. The model results showed swash zone shear stress is a dome-shaped function of distance across the beach-face thereby controlling gutter depth. Further, high-speed sheet flows characterised by periodic, shore-normal, high and low speed streaks alongshore are thought to be implicated in the mechanism controlling gutter spacing. However, in any situation, the specific spacing of gutters is moderated by both the local sheet flow characteristics and the larger-scale morphological forcing. Together these factors indicate that gutter spacing is an emergent property which makes spacing unpredictable.

Keywords: Gutter-casts; gutters, grooves, runnels, beach-face, wave modelling

1. Introduction

Linear erosional bedforms cut into soft bedrock are reported widely with different descriptive names (e.g. furrows, grooves, gutters, runnels). The term groove is adopted in the following text. Grooves are usually relatively long, straight or weakly sinuous but otherwise parallel [1], and spaced more-or-less regularly across fairly plane surfaces at intervals of a few decimetres to a few metres. The incisions may be deep (<1 m) with vertical and overhanging sides [14].

Despite their common occurrence in the rock record, grooves can have disparate origins and so it is important for environmental reconstruction to detail modern examples to aid discrimination of the depositional context. Shore-normal grooves have been reported for littoral and sub-littoral locations and have been ascribed to erosion of the substratum by reversing wave-induced currents [3], especially during storms [13].

In the case of modern beaches, the published examples are developed on soft bedrock. [1] ascribes the origin of grooves to wave swash,

whereas [8] relates them to back-swash. To date researchers are unable to account for the spacing of beach-face grooves.

It is hypothesised here that groove morphology reflects the wave-induced sheet flow processes within the swash zone. While mobile beach sediments may assist in the erosion of the grooves [10] fluid stressing alone in high-velocity flows is capable of eroding firm siltstone. However, shear forces $O(100 \text{ N/m}^2)$ are required to scour compacted formations and so abrasion by bedload must cause erosion as well as fluid stressing.

Here grooves formed in a soft sandstone on a steep beach-face subsequent to storm wave action are reported. Although no hydrodynamic data were collected during the event, simulations of wave run-up on the beach-face for known off-shore conditions are placed within a theoretical framework and are used to propose a model for groove formation.

2. Field site

An aerial view of the study area in Figure 1 from July 2014 shows the site after the winter storms of 2013-

2014. Highlighted on the image are beach profile locations referred to below, the realignment breach location, gravel overwash deposits and the area of grooves examined in this paper.

The steep beach-face consists of sandstone in three Divisions of the Bracklesham shallow marine beds of Eocene age [4], with a thin covering of shingle. The siltstone usually is exposed only locally as a steep slope, being overlain by a variable thickness of modern shingle with sand cover to seaward on the lower beach-face. The shingle cover rises to circa 5.4 m Ordinance Datum Newlyn (ODN).



Figure 1: Aerial view of the Environment Agency Medmerry managed realignment breach site, July, 2014 (Channel Coastal Observatory, UK, CCO).

At Medmerry, the modelled spring and neap tidal ranges are around 4.9 m and 2.7 m, respectively and offshore tidal currents at flow predominantly eastwards and south-eastwards. The offshore wave climate is dominated by waves from the south and south-west with episodes of less energetic waves from the south-east. Maximum annual significant wave heights of 2.85 m are reported for the shoreline west of Selsey Bill, decreasing westward to 1.24 m near West Wittering.

From mid-December to early January 2013/2014, the UK experienced a period of extreme weather as a series of major winter storms affected the south coast of England [12]. These storms were characterised by a combination of large wind-generated and swell waves and some occurred during high spring tides. Winds of 130 km/h occurred at Isle of Wight 54 km to the west of Medmerry. Exceptionally high near-shore wind-waves ($H_s=6$ m) were recorded on the 5th January 2014 and these storm conditions persisted periodically through to mid-February 2014. The period from mid-December 2013 to mid-February 2014 experienced at least 12 major winter storms, and, when considered overall, this was the stormiest period of weather the UK has experienced for 20 years.

As a consequence, the beach surface was stripped of sediment and grooves were formed as a result of erosive wave action (Figure 2). Owing to the steepness of the beach-face and the offshore transport of sediment little shingle and sand is retained in the grooves.



Figure 2: View looking seaward from the top of a portion of the grooved beach-face. Remnants of shingle cover remain as isolated blocks (two examples arrowed at the top of the photo) or small groups of pebbles (lower right).

3. Method

3.1 Wave modelling

Wave modelling was undertaken using the one-layer, depth-averaged, non-hydrostatic extension to the XBeach model, XBeach-G [11]. In the model build process the objective was to reproduce as accurately as possible with available data, the pre- and post-storm beach profiles and to link these seamlessly with the offshore bathymetry.

Swath bathymetry for the area from 2013, the location of the Bracklesham Bay wave buoy, the approximate location of mean high water spring tide level (MHWS) and the Medmerry breach are shown in Figure 3. The maximum and minimum measured offshore water depth is around -16 m and 1 m ODN, respectively.

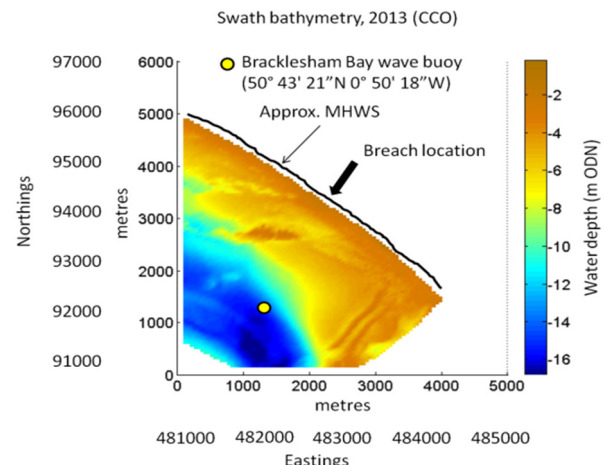


Fig. 3: Swath bathymetry from 2013 showing the location of the Bracklesham Bay wave buoy (CCO), MHWS and Medmerry breach.

To illustrate the impact of the 2013-2014 winter storms, Figure 4 shows beach profile SUSS56 (Figure 1) measured on: (a) 24th September, 2013 before the start of the winter storms, and (b) 1 May, 2014 after the winter storms. Figure 4 shows severe erosion during the period 24 September 2013 to 1 May, 2014 with a landward recession of around 25 m and crest lowering of 1.5 m. However, around the location of MLW, the beach elevation shows much less change (typically < 0.2 m). Thin gravel deposits normally present on the beach face were transported landwards to form overwash fan deposits. The removal of the sediment resulted in the exposure of the Bracklesham Beds to tidal and wave action (Figure 5).

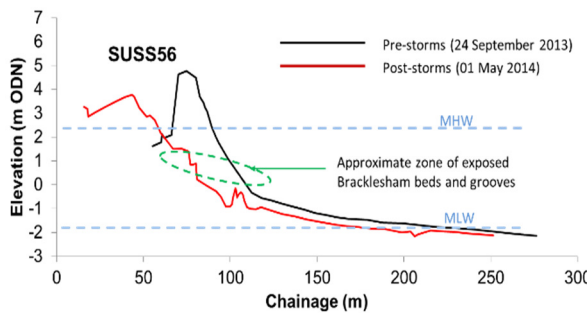


Figure 4: Pre- and post-storm beach profile SUSS56 showing MHW and MLW (CCO)



Figure 5: Aerial view of the Medmerry breach site showing areas of exposed grooves in the Bracklesham beds and gravel overwash fans resulting from the 2013-2014 winter storms.

To ensure accurate wave transformations the XBeach-G model bathymetry was created by extending profile SUSS56 offshore to the Bracklesham Bay wave buoy location (Figure 3) and extracting the profile data at 5m intervals to produce a seamless 1D XBeach model profile extending for approximately 3000 m from an offshore location around -15m ODN to the beach crest at around +5m ODN. Since the evolving characteristics of the beach profile during the period between surveys is unknown, for the purpose of the modelling study only the pre-storm profiles are used in the modelling study.

Measured tide and wave conditions during the period 1 December 2013 to 10 February 2014 are shown in Figure 6. While the exact characteristics of the events resulting in the grooves formation are unknown, it is possible to quantify a number of key hydrodynamic and wave parameters pertaining during selected storm events. In this way an assessment can be made that links the local, near-shore wave and hydrodynamic conditions during storm events with the grooves and thus adds further understanding of their origin and formation.

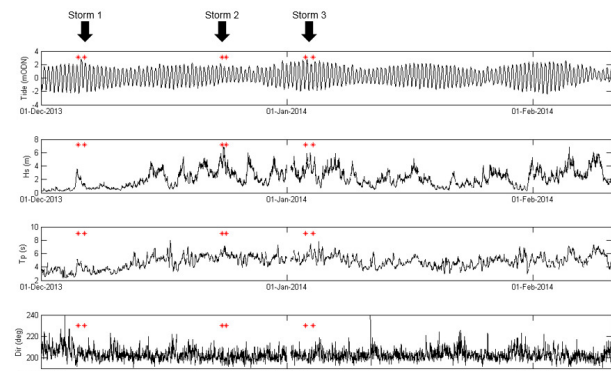


Figure 6: Tide and wave conditions 1 December 2013 to 10 February 2014 showing the 3 storm periods simulated in the XBeach-G models (from CCO and NSLTF)

The 3 storm periods that provide a range of extreme events in Figure 6 include: (a) Storm 1 with moderate waves coincident with an exceptionally high tide; (b) Storm 2 with exceptionally high waves occurring during neap tides; and (c) Storm 3 with high waves occurring during spring tides. The characteristics of these storms are summarised in Table 1 which defines minimum and maximum values for tidal elevation, h , significant wave height, H_s , peak wave period, T_p , and mean wave direction, θ .

For a given storm period, water elevation time-series and time-varying JONSWAP spectra were applied at the offshore boundary of the model. The cross-shore boundaries were open and the beach was defined as being reflective. The median grain size of the beach sediments was set to 1 cm and other model parameters settings followed the fully validated XBeach 'factory' setting detailed in [6]. All XBeach-G outputs were sampled at 1s intervals.

	h (m)		Hs (m)		Tp (s)		θ (deg)
	Min.	Max.	Min.	Max.	Min.	Max.	Mean
1	-2.33	2.83	1.0	2.5	3.3	4.9	206
2	-0.67	1.74	2.7	6.9	5.6	7.1	202
3	-1.89	2.76	2.8	6.0	4.8	7.5	197

Table 1: Characteristics of the three storm events selected for the study.

3.2 Terrestrial laser scanning of groove morphology

A Leica P20 Terrestrial Laser Scanner (TLS) was deployed during low tide on the lower sandy foreshore 29th January 2014, looking up the beach towards the grooves. A single scan of the grooves over an area of approximately 10 x 10 m was made using a point spacing of 3.1 mm at a 10 m distance, with the highest quality setting giving a mean point spacing of ~ 2 mm and a mean point density of ~ 2 M points per m². The few deepest parts of the grooves oblique to the TLS location were occluded.

Following post-processing the point cloud was cropped to a 4.3 x 10 m area directly in front of the TLS instrument to allow more accurate estimates of runnel depths to be derived in the areas with least occlusion (e.g. Figure 7). The data were imported into ArcGIS and interpolated to form a surface using Delaunay triangulation. A series of 9 equidistantly spaced transects, perpendicular to the orientation of the grooves, were established across the surface at 1m spacing to extract the underlying topographic data. The resultant profiles of ridge-groove features were analysed to derive metrics of groove spacing (B) and groove depth (D).

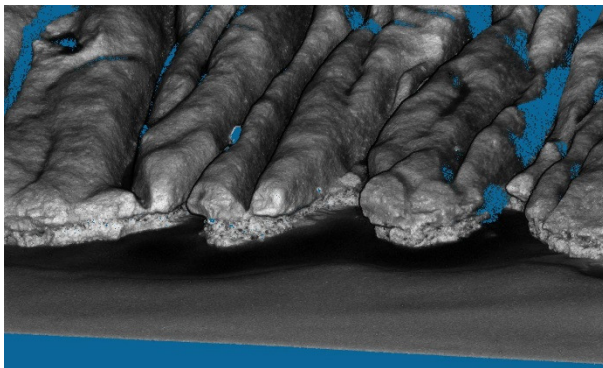


Figure 7: Close-up oblique view of the wave-eroded lowest termination of grooves where they are replaced by sand to seaward. Blue hatching represents residual sand in the grooves.

4. Results

4.1 XBeach-G modelling

Since the hypothesis for groove formation proposed here is predicated on erosion by incident waves, the analysis of XBeach-G results for this study has focussed on predicted peak and time-averaged bed shear stresses at cross-shore locations on the shoreface. Typifying results from all XBeach-G model runs, and thus providing a useful example with which to demonstrate how the model results support the groove formation hypothesis, XBeach-G results from the first 6 hours of the Storm 3 simulation, hereafter termed S36, are shown in Fig. 9. This figure shows a rising spring tide plus surge in the range -0.55 m to 2.76 m ODN and offshore significant wave heights and peak wave periods in

the ranges 5.2 m to 5.7 m and 4.9 s to 6.3 s, respectively.

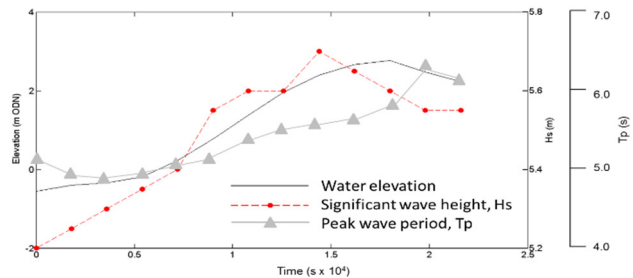


Figure 8: Hydrodynamic and wave conditions during storm period S36.

Individual swash and backwash events associated with incident waves were identified in the Xbeach-G time-series using a zero down-crossing time-series analysis. By assuming a constant drag coefficient, Cd, of 0.0025, the bed shear stress was obtained using the quadratic stress law

$$\tau = \rho_w \cdot Cd \cdot U^2 \quad (1)$$

for swash (τ_{sw}) and backwash (τ_{bw}) events, where ρ_w is the assumed density of sea water (1023 kg/m³) and U is the depth-averaged instantaneous flow velocity predicted by XBeach-G. In the model positive and negative U values denote swash and backwash flows, respectively. While it could be argued that the chosen Cd value is arbitrary, it is a value recommended by Soulsby (1997) in situations where no information is available, or where only a rough estimate is required. Further, since an important aspect of the present study is to establish the general characteristics of the cross-shore wave-induced bed shear stress distribution and its relationship, if any, to the observed groove morphology, the use of this Cd value will not affect this spatial interpretation of the XBeach-G model results.

20s time-averaged bed shear stress time-series from S36 spanning approximately 6 hours were extracted from Xbeach-G at the 12 cross-shore locations shown in Figure 9. Xbeach-G data were processed to obtain mean bed shear stress averaged over approximately 6 hours, τ_{mean} , and peak bed shear stress, τ_{max} , values at the XBeach-G cross-shore data extraction locations between X = 1830 m and X = 1857.5 m (Figure 10).

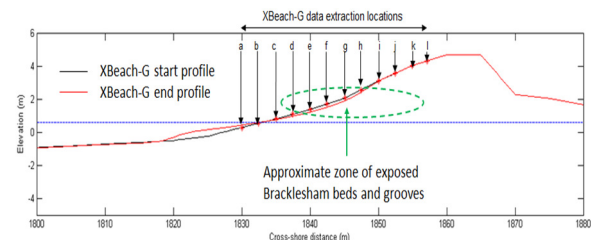


Figure 9: Location of XBeach-G data extraction points at 2.6 m spacing between cross-shore distances from 1830

m to 1857.5 m. The black and red lines denote the beach profile at the start and end of the XBeach-G simulation, respectively.

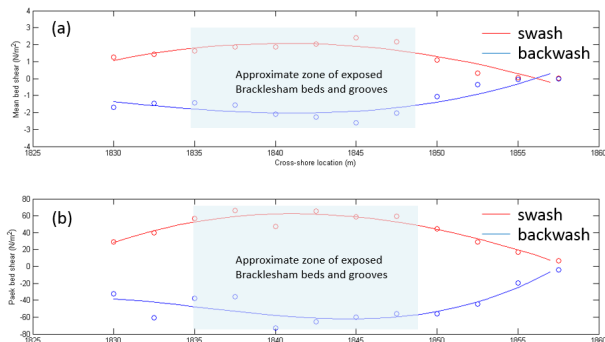


Figure 10: XBeach-G derived cross-shore distribution of bed shear stress for swash and backwash events over a 30-minute period: (a) mean values, τ_{mean} ; and (b) peak values, τ_{max} .

The temporal and spatial distribution of predicted bed shear stress for run S36 at all 12 cross-shore locations (Figure 9) is shown in Figure 11 for the total bed shear stress (combined swash and backwash events) and for swash and backwash events separately.

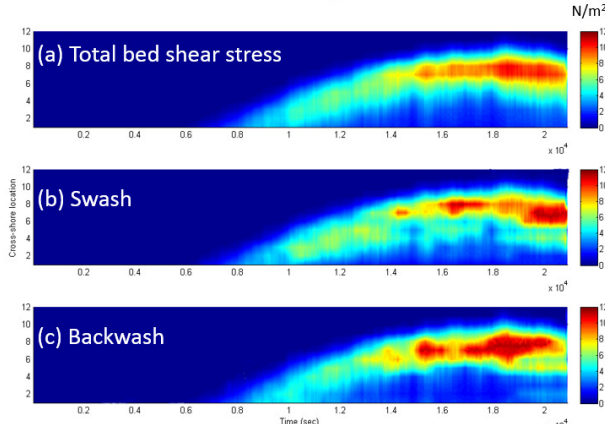


Figure 11: XBeach-G derived temporal and cross-shore distributions of: (a) combined swash and backwash bed shear stress; (b) swash-only bed shear stress; and (c) backwash-only bed shear stress event.

Noting that the critical shear stress to erode fully consolidated mud is around 9.2 N/m² [5], Figure 11 shows that shear stresses between sample locations e and g (Fig. 9) exceed these threshold values for the latter part of the S36 model run and thus erosion of the Bracklesham Beds in this region of the beach profile would be expected. Figure 11 shows also that shear stress values decrease seaward and landward from peak values around location f and thus the degree of erosion would also be expected to decrease correspondingly. However, the abrasive contribution to erosion associated with sediment held within the wave swash and backwash flows is not accounted for in this interpretation of the XBeach-G simulation. Given the slightly higher bed shear stress values

associated with the backwash flows, it is expected that backwash would tend to be marginally more effective at eroding the Bracklesham Beds than the swash.

4.2 Groove morphology

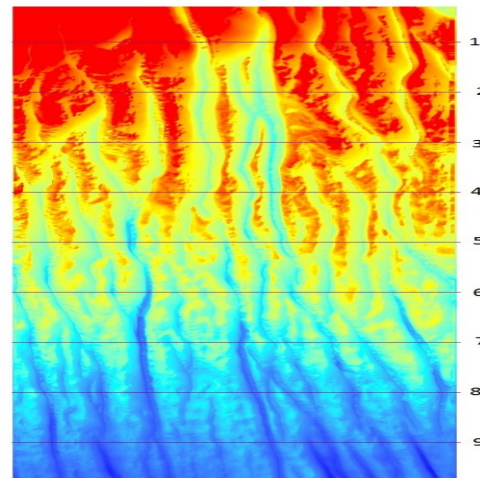


Figure 12: Vertical view of the grooves. The horizontal field of view is 4.3m. False colouring reflects the offshore trend from high elevations (red hue) to low elevations (blue hue). Numbered profile lines are those used to extract topographic data (Table 2).

Profile	1	2	3	4	5	6	7	8	9	Mean	SD
N	8	8	8	10	12	13	13	12	12	10.6	2.18
B _{mean}	0.49	0.49	0.37	0.41	0.34	0.31	0.31	0.35	0.36	0.38	0.12
B _{SD}	0.19	0.12	0.12	0.14	0.08	0.04	0.15	0.13	0.11	-	-
D _{mean}	0.24	0.17	0.17	0.15	0.13	0.11	0.08	0.07	0.14	0.13	0.06
D _{SD}	0.09	0.07	0.09	0.06	0.07	0.06	0.06	0.04	0.03	-	-

Table 2: Summary statistics for the nine sampling lines in Figure 12. N is the number of samples, B is groove spacing and D is groove depth.

Analysis of the data show that there is no discernible variation in groove morphology attributable to differences in the sedimentology. The density of grooves increases down-slope, as the spacing (B) of the troughs declines in the same direction. Some grooves extend the full height of the beach-face. Occasional, bifurcations in grooves occur both up-slope and down-slope. A few terminate downslope before the base is reached, but usually short, closely-spaced grooves occur on the lower beach-face.

The best fit for the groove spacing, B, is a negative logarithmic function of distance down slope but there is no significant change in the standard deviation (SD) of the spacing with distance X.

$$B = -0.0823 \ln(X) + 0.4971, (R^2 = 0.74) \quad (2)$$

The best fit for the groove depth, D, is a negative linear function of distance down slope and there is

a significant linear trend in the decrease of the SD of the depths in the same direction.

$$D = -0.0211 (X) + 0.2365, \quad (R^2 = 0.95) \quad (3)$$

The up-slope terminations of the grooves are usually abrupt with a planar siltstone surface further up-slope close to the margin of the stripped beach shingle.

5. Discussion

It was hypothesised above that groove morphology reflects the beach-face wave-induced sheet flow processes within the swash zone and that mobile shingle and sand probable assist in the erosion of the grooves. Further, once small grooves form, the evolving bathymetry must increasingly constrain the local erosive flow within the groove and ‘lock’ grooves into place where they can grow bigger.

The abrupt up-slope terminations to deep grooves and the steady reduction in the groove depths down the beach-face may results from the cross-shore wave-induce shear stress. [2] and [15] demonstrate that wave height decreases rapidly across the beach whereas the set-up increases up the beach-face. Significantly, both the back-swash velocity and the turbulent kinetic energy (TKE) peak about 2/3 of the way up the beach where the back-swash meets the incoming swash. TKE decreases rapidly at higher elevations. The Xbeach-G model results support these observations.

To explain groove spacing it has been argued that: (a) incipient topographic lows in the beach profile are amplified by attracting and accelerating swash so that the depressions are enhanced [9]; and (b) the front of swash flow inherently forms periodic salients of faster and slower flow which leads to differential erosion and deposition along the beach-face that reflects the initial salient structure [7]. These different views are possibly reconciled by [16] who argue that beach-face patterns are due to self-organization of the sediment surface due to the local flow crossing a plane bed. However, while self-organised patterns may be related to forcing by wave height and storm duration, they cannot account for specific bedform spacing.

6. References

- [1] Allen, J.R.L., 1982, Sedimentary Structures: their Character and Physical Basis, Vol II, Elsevier, Amsterdam, 663pp.
- [2] Baldock, T.E., Holmes, P. & Horn, P., 1997, Low frequency swash motion induced by wave grouping. Coastal Engineering, 32, 197-222.
- [3] Beukes, N.J., 1996. Sole marks and combined-flow storm event beds in the Brixton Formation of the siliciclastic Archean Witwatersrand supergroup, South Africa. Journal of Sedimentary Research, 66, 567-576.
- [4] Curry, D., King, A.D., King, C. & Stinton, F.C. 1977. The Bracklesham Beds (Eocene) of Bracklesham Bay and Selsey, Sussex. Proceedings of the Geologists' Association, 88: 243-254.
- [5] Dean, R.G. & Dalrymple, R.A., 2002, Coastal Processes: with Engineering Applications. Cambridge University Press, Cambridge, UK.
- [6] Deltires, 2015. XBeach Manual. 145pp. http://oss.deltares.nl/documents/48999/49476/XBeach_manual_11032015.pdf.
- [7] Gorycki, M.A., 1973. Sheetflood structure: mechanism of beach cusp formation and related phenomena. Journal of Geology, 81, 109-117.
- [8] Hawkes, D.D., 1962. Erosion of tidal flats near Georgetown, British Guiana. Nature, 196, 128-130.
- [9] Hughes M.G. & Turner, I., 1999. Handbook of Beach and Shoreface Morphodynamics. Short, A.D., (ed.), 1999. Chichester: Wiley pp. 119-144. ISBN 0-471-965707
- [10] Kamphuis, J.W., 1990. Influence of sand or gravel on the erosion of cohesive sediment. Journal of Hydraulic Research, 28(1), pp.43-53.
- [11] McCall, R.T., Masselink, G., Poate, T.G., Roelvink, J.A., Almeida, L.P., Davidson, M. & Russell, P.E., 2015. Modelling storm hydrodynamics on gravel beaches with XBeach-G. Coastal Engineering, 103, 52–66.
- [12] Masselink, G., Scott, T., Conley, D., Davidson, M. & Russell, P., 2015. Regional variability in Atlantic storm response along the southwest coast of England. Proceedings Coastal Sediments, ASCE, San Diego, USA.
- [13] Plint, A.G. & Nummendal, D., 2000. The falling stage systems tract: recognition and importance in sequence stratigraphic analysis. Pp. 1-17 In: D. Hutt and R.L. Gawthorpe (Eds.) Sedimentary Responses to Forced Regressions. Special Publication 172, The Geological Society of London.
- [14] Shank, J.A. & Plint, A.G., 2013. Allostratigraphy of the Upper Cretaceous Cardium Formation in subsurface and outcrop in southern Alberta, and correlation to equivalent strata in northwestern Montana. Bulletin of Canadian Petroleum Geology, 61: 1-40.
- [15] Shin, S. & Cox, D., 2006. Laboratory observations of inner surf and swash-zone hydrodynamics on a steep slope. Continental Shelf Research, 26, 561–573.
- [16] Werner, B.T. & Fink, T.M., 1993. Beach cusps as self-organized patterns. Science, 260, 968-971.